Journal of Petroleum
Science and Technology

Performance of Carboxymethyl Cellulose Produced from Cocoa Pod Husk as Fluid Loss Control Agent at High Temperatures and Variable (Low and High) Differential Pressure Conditions-Part 1

Wilberforce Nkrumah Aggrey[1,2]*, Nana Yaw Asiedu[3], Bennet Nii Tackie-Otoo[4], Stephen Adjei[4], and Emmanuel Mensah-Bonsu[2]

[1]Department of Petroleum Engineering, Kwame Nkrumah University of Science and Technology, Kumasi, PMD, Ghana
[2]Petroleum Research Laboratories-Drilling Fluids Engineering, Kwame Nkrumah University of Science and Technology, Kumasi, PMD, Ghana
[3]Department of Chemical Engineering, Kwame Nkrumah University of Science and Technology, Kumasi, PMD, Ghana
[4]Department of Petroleum Engineering, All Nations University College, Koforidua, Ghana

ABSTRACT

Environmental concerns and cost associated with drilling operations have made us promote the application of biodegradable and renewable drilling fluid additives, particularly at high temperature. In this study, sodium carboxymethyl cellulose (NaCMC) synthesized from cocoa pod husk (cocoa NaCMC) was tested as a filtration agent at high temperature and differential pressure conditions. Moreover, eight mud samples containing various fluid-loss additives were tested. The Filtration test was performed using the permeability plugging tester at 248 °F temperature and 100 psi and 300 psi differential pressures with ceramic discs 10 µm and 90 µm. In addition, the degree filtration agents affect the drilling mud's rheological parameters were estimated. Also, thermal degradability of the sample was also studied. The results showed that filtration control performance at high temperature and low/high differential pressure was improved by decreasing particle size and increasing concentration. Using the cocoa NaCMC was proved to be a better filtration agent at high-temperature conditions with a high thermal degradability. Finally, the obtained results indicated that the filtration control performance declined in higher permeable formation. Moreover, the drilling fluid's rheological properties were improved by the cocoa NaCMC, and it was comparable to the industrial PAC.

Keywords: Cocoa Pod Husk, Cellulose, Sodium Carboxymethyl Cellulose, Filtration Characteristics, Drilling Fluids

***Corresponding author**
Wilberforce Nkrumah Aggrey
Email: kwesiobi@gmail.com
Tel: +233 05 0804 7368
Fax: +233 05 0804 7368

Article history
Received: November 29, 2018
Received in revised form: May 31, 2019
Accepted: June 9, 2019
Available online: December 20, 2019
DOI: 10.22078/jpst.2019.3550.1570

INTRODUCTION

An important part of drilling operations in the oil and gas industry is the drilling mud or fluid. It performs various functions including transporting drill cuttings to the surface, lubricating, and cooling the drill bit, sustaining the stability of wellbore and regulating formation pressure [1]. Therefore, success in drilling operations requires that drilling fluids possess desirable qualities which depend on their rheological and fluid filtration properties [2]. Among these qualities of drilling fluid, satisfactory filtration control is required to avoid drilling issues that include extreme drag and torque, lost circulation, formation damage, and wellbore instability which affects well productivity [2–4]. In view of these challenges, several fluid loss agents and additives have been formulated and synthesized for various applications in invert, oil, and water-based drilling fluids [5–11].

Various components are applied to water-based drilling muds to improve the filtration characteristics and rheological parameters [12]. Bentonite is the commonly used component in drilling muds to increase viscosity and regulate fluid loss because of its excellent colloidal properties. Moreover, conventional drilling fluids require a large amount of bentonite to achieve desirable rheological and filtration properties [13]. Nonetheless, in higher concentrations, bentonite possesses drilling problems as mentioned above [2]. Therefore, drilling fluids are augmented by various polymers as viscosity modifiers and fluid loss control additives. Polymers commonly used in drilling fluids are cellulose derivatives of carboxymethyl cellulose (CMC) and polyanionic cellulose (PAC), guar gum, and xanthan gum. Moreover, cellulose derivatives are the most preferred because they are biodegradable and compatible with other components of drilling fluid. Although it has been reported by Okorie and Julius [9] in their review paper which explains “how some agro-waste has been used for the synthesis and design of lost control agents.” It is important to note that differences in texture, thermal stability, compressive strength, cost and their effects on the pay zone are factors that influence how and where the LCMs are deployed. In addition, finding a fluid loss control agent that is cheap, stable, and strong and has a low effect on the pay zones is desirable, and several studies must be conducted and tested for such fluid loss agents.

Another challenge in drilling fluid technology is drilling in high permeability reservoirs particularly sandstone formations with high permeability zones and high temperatures which are to be plugged during drilling and completion activities without degradation of the polymer material. Such formations require a mat-like bridge on the wall of the borehole to combat lost circulation [9].

Drilling and completions problems intensify in deep drilling and completion because of the rise in temperature and pressure which leads to degradation of drilling and completion fluid properties [14]. This degradation of fluid properties is mainly because of the flocculation, degradation, and instability of bentonite at HPHT conditions [13, 15]. In addition, polymers decompose, and they are unstable at HPHT conditions [3, 16]. Oil-based mud was the choice of drilling fluid in these hostile environments for years because they are thermally stable up to 500 ^{o}F. Nevertheless, environmental legislation has increased restrictions on their usage, and they are totally prohibited in some countries [17]. This makes the use of polymers

in water-based drilling fluids indispensable (or essential). There are alternative synthetic polymers that are stable at high-temperature conditions, but these polymers are expensive and have associated environmental concerns too [16].

There are several works in literature where plant wastes have been valorized to reduce the cost of drilling operations yet they are unable to meet other fluid loss criteria such as stability, mat-like plugging nature for high sandstone permeability formations, thermal stability, and compressive strength. Converting plant wastes into needful products presents a lot of socio-economic issues [18]. In these studies, plant wastes are either used in their raw state, or cellulose derivatives are extracted from them. Various plant wastes have been used in this regard: agarwood waste [19], rice husk [4], corn starch [20], peanut hull [21], sugarcane [22], corn cobs, coconut shell [23], and wood wastes [24].

In this paper, the results of laboratory and experimental work which have been carried out are reported; in addition, this study reports the first part of the results at considerably low and high differential pressure and high-temperature regime of sodium carboxymethyl cellulose synthesized from cocoa pod husk and used as a filtration agent in water-based mud to answer the challenges raised in this literature. The focus of this work is to analyze the workability of this NaCMC synthesized from cocoa pod husk as a filtration agent at high temperatures without thermal degradability and its effect on the pay zones (permeability) as well as using the morphological sequence of the synthesized fluid loss agent comparing it with the industrial premium; polyanionic cellulose (PAC).

EXPERIMENTAL PROCEDURE

Materials

Wyoming sodium bentonite was supplied by Kenon Drilling Services (Takoradi, Ghana), and industrial polyanionic cellulose (PAC) was supplied by Baker Hughes (Takoradi, Ghana). Moreover, sodium hydroxide (≥99% acidimetric), isopropanol (99% purity), methanol (99% purity), and ethanol (≥95% purity) were supplied by Research – Lab Fine Chemicals Industries. Sodium mono chloroacetate (≥98% acidimetric), glacial acetic acid (99% purity), and phenolphthalein were purchased from LabChem. The necessary chemicals were at analytical levels and used as obtained.

Cellulose Extraction from Cocoa Husk

Fresh cocoa pods were obtained from Jinijini in the Brong Ahafo region of Ghana. The pods were dried for 2 weeks, crushed into smaller sizes, and blended into powder form. The powder was then sieved using the Retsch sieve analysis machine for 15 minutes. The various particle sizes were collected and weighed. The machine has five sieves with sizes 500 µm, 250 µm, 125 µm, 63 µm, and 25 µm.

100 grams of cocoa husk powder were dissolved in 2% w/v sodium hydroxide (NaOH) in a beaker. The resulting mixture was heated in a water bath at 80 °C for 3 hours, and it thoroughly washed under distilled water until the pH was approximately neutral. It was then bleached with 500 ml Mirazone bleach containing 7% of sodium hypochlorite at 80 °C under mechanical stirring for 15 minutes. The mixture was later treated with 1L 12% w/v NaOH solution and heated at 80 °C for an hour. Final bleaching was done to remove the remaining lignin and hemicellulose and also to purify the cellulose.

The extracted cellulose was washed thoroughly with distilled water and dried in an oven at 60 °C for 24 hours. In Appendix 1, a photo gallery of the conversion of cellulose from the crushed cocoa husk is shown.

Synthesis of Cocoa Sodium Carboxymethyl Cellulose

Extraction of crude cellulose from cocoa pod husk was done similar to the procedure used by Hutomo et al [25]. The extracted cellulose was insoluble in the drilling fluid formulated; therefore, it was converted into a soluble cellulose derivative, sodium carboxymethyl cellulose (NaCMC), by attaching a carboxymethyl (-CH_2-COOH) side chain unto the cellulose backbone. Moreover, NaCMC synthesis involves reacting cellulose with chloroacetic acid in the presence of a base [26]. Synthesis of NaCMC was done according to the method of Hutomo et al [25]. The followed procedure is fully described below.

30 ml of NaOH and 270 ml of isopropanol were added to 45 grams of the extracted cellulose in a beaker. The mixture was mechanically stirred and allowed to stand for 30 min at room temperature. Afterwards, 10.8 grams of sodium monochloroacetic acid was added to the pre-treated cellulose with continuous stirring for 90 min. The mixture was covered with aluminum foil and kept in an oven at 55 °C for 180 min. The slurry was neutralized with glacial acetic acid and then filtered. The sodium carboxymethyl cellulose produced was washed with 300 ml of ethanol to remove undesirable salts, followed by a methanol wash to remove remaining impurities and dried in an oven at 55 °C for an hour. Appendix 2 shows a photo gallery of the conversion of extracted cocoa cellulose into cocoa sodium carboxymethyl cellulose.

FT-IR Spectroscopy of Extracted Cellulose and Sodium Carboxymethyl Cellulose

FTIR study into the composition of the extracted cellulose and the synthesized NaCMC was conducted using a Perkin Elmer UATR Spectrum Two FTIR spectrometer to record the infrared spectra of the dried extracted cellulose and NaCMC. The transition was measured at the wavenumber region of 4000-400 cm^{-1} having a resolution of 4 cm^{-1}.

Drilling Fluid Formulation

Water-based drilling fluids consisting of 20 g of bentonite (main component for viscosity and filtration control in drilling fluids), 350 ml of water and 0.4 gram NaOH, 0.5 gram KCl, and 5 gram barite were prepared according to API Specification 13A [27]. In addition, different drilling fluid samples were prepared as shown in Table 1. This was to investigate the performance of the extracted cellulose and the synthesized NaCMC at different particle sizes and mass concentrations. The performances of the samples were compared to that of a drilling mud formulation having no additive to control loss of fluid and a formulation with industrial polyanionic cellulose as a fluid loss control additive.

Table 1: Drilling formulation samples and their components.

Sample	Water	Bentonite	Additive
A	350 ml	20 g	No fluid loss control additive
B	350 ml	20 g	<25 µm of Industrial PAC
C	350 ml	20 g	<63 µm of cocoa NaCMC
D	350 ml	20 g	<125 µm of cocoa NaCMC
E	350 ml	20 g	<250 µm of cocoa NaCMC
G	350 ml	20 g	<63 µm of extracted cellulose
H	350 ml	20 g	<25 µm of cocoa NaCMC
I	350 ml	20 g	<25 µm of extracted cellulose

High Pressure and Low and High Differential Pressure Filtration Test

The test was done at a temperature of 120 °C and differential pressures of 100 and 300 psi deploying Fan permeability plugging tester. The test was done with a ceramic disc of 10 µm and 90 µm mean pore throat diameters thus simulating low and high permeability formations respectively. The equipment is made to mimic downhole fluid loss at the dynamic condition, and the ceramic disc closely replicates the structure of formation. This, therefore, gives a better depiction of filtration process downhole.

The filtration characteristics can be derived from the volume of filtrate collected at 7.5 and 30 minute intervals according to Equations 1 to 3 [28]:

Permeability plugging tester value (PPTV)

$$(PPTV) = 2 \times Vol_{30\ \min} \quad (1)$$

$$(SL) = 2 \times \left[Vol_{7.5\ \min} - \left(Vol_{30\ \min} - Vol_{7.5\ \min} \right) \right] \quad (2)$$

$$(SFR) = 2 \times \frac{\left(Vol_{30\ \min} - Vol_{7.5\ \min} \right)}{2.739} \quad (3)$$

where $Vol_{7.5}$ min and Vol_{30} min are the total filtrates obtained in 7.5 min and 30 min respectively.

After the 30 min, the filter cake's thickness on the ceramic disc was measured. The dried filter cake's thickness formed at 30 min was then taken. The samples tested were samples A, B, C, D, E, G, H, and I. Samples G and I were insoluble in the drilling mud. This brought the need for CMC conversion.

Rheological Testing

The effects of the filtration agents on the rheology of the mud formulation were evaluated by using the Fann rheometer model 286. Drilling muds are commonly Non-Newtonian and exhibit pseudo-plastic behavior [29]. They exhibit rheological behavior between the Bingham Plastic and the Power Law models [1]. Therefore, their pseudoplastic behavior is most described by using these two rheological models. The rheological parameters were obtained above a shear rate region of 10.2–1022 s^{-1} using these models. Only samples A, B, C, and I were used in this test. According to the Bingham Plastic Model [29], the following equations (Equations 4, 5, and 6) are governed:

$$\text{Apparent viscosity}(\mu_\alpha) = \frac{\theta_{600}}{2} \quad (4)$$

$$\text{Plastic viscosity}\left(\mu_p\right) = \theta_{600} - \theta_{300} \quad (5)$$

$$\text{Yield point}\left(\tau_y\right) = \theta_{300} - \mu_p \quad (6)$$

where θ_{300} and θ_{600} are 300 and 600 rpm dial readings respectively. The gel strengths of the drilling muds were also obtained as GS10 sec and GS10 min by recording the maximal dial deflection at a 3 rpm when the drilling fluids have remained still for 10 sec and 10 min respectively.

According to the Power Law Model [1], Equation 7 is governed:

$$\tau = K \gamma^n \quad (7)$$

where,

τ = shear stress,

γ = shear rate,

n = flow index, and

K = consistency index.

Moreover, n and K are derived from Equations 8 and 9:

$$n = 3.32 \log\left(\frac{\theta_{600}}{\theta_{300}}\right) \quad (8)$$

$$K = \frac{\theta_{600}}{1022^n} \quad (9)$$

SEM and Thermal Degradation Studies

SEM images of the cocoa cellulose and PAC were obtained by Hitachi SU8010 ultra-high resolution equipment.

Figure 1 (a and b) represents the SEM images of the cocoa CMC and industrial PAC respectively.

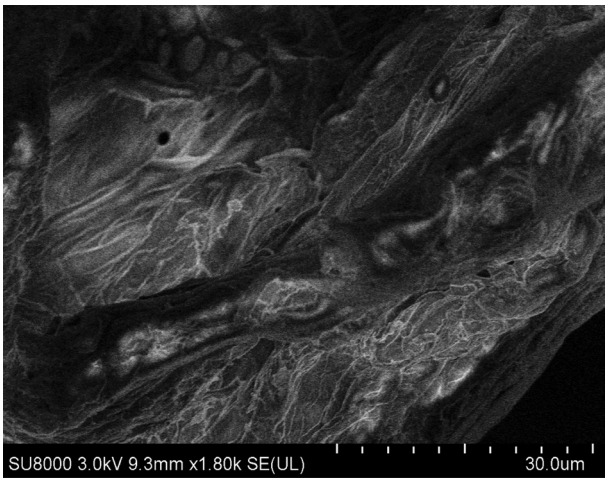

Figure 1 (a): SEM image of Cocoa CMC.

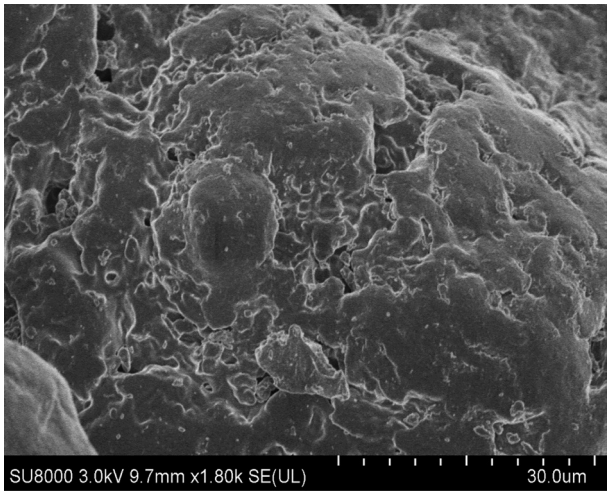

Figure 1 (b): SEM image of industrial PAC.

Both images were taken at 30 µm resolution. TGA pyrolysis (under argon) was set to operate from room temperature (20 °C) to 800 °C at a low heating rate (10 °C/min). The thermogravimetric (TG) and the derivative thermogravimetric (DTG) plots of the cocoa pod husks are shown in Figure 2 (a and b) respectively.

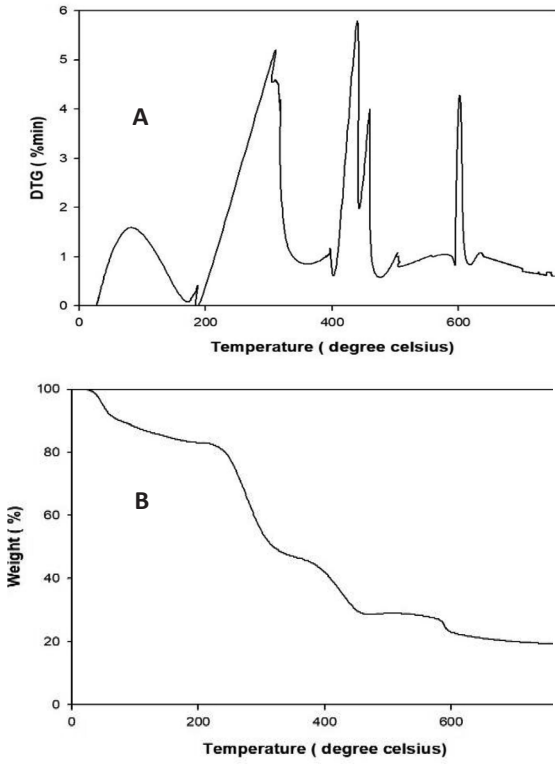

Figure 2: (a) DTG plot for the cocoa NaCMC (b) TGA plot for cocoa NaCMC.

RESULTS AND DISCUSSION

Extracted Cellulose and Sodium Carboxymethyl Cellulose Characterization

Figures 3 and 4 present results of the IR spectra of the extracted cellulose and NaCMC respectively. Broad adsorption band at 3327 cm^{-1} is because of an H-bonded and OH stretch which is peculiar to the hydroxyl group [30].

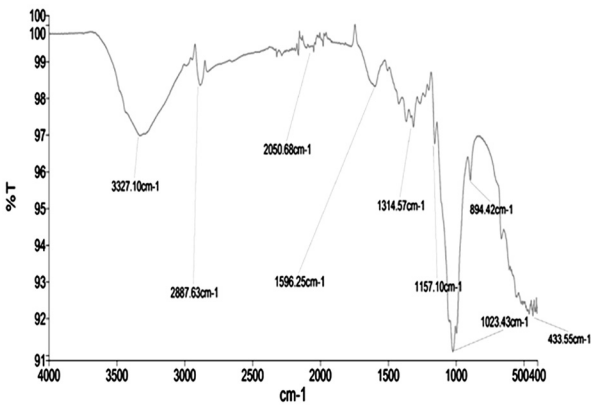

Figure 3: FTIR spectrum graph of extracted cellulose.

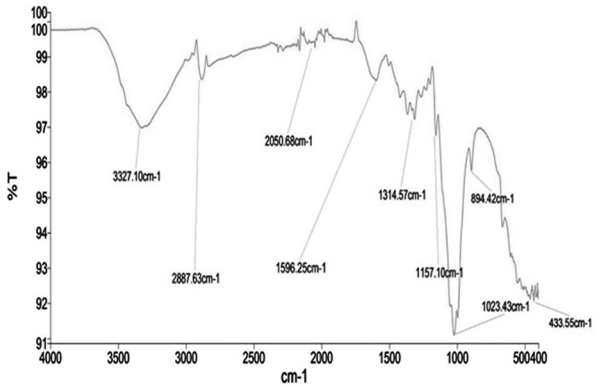

Figure 4: FTIR Spectrum Graph of NaCMC.

The presence of the hydroxyl group the primary functional group of cellulose is indicative of the presence of cellulose in the extract. Also, in Figures 3 and 4, peaks at wavenumber 2887.63 cm^{-1} and 2878.51 cm^{-1} are respectively seen. This is due to the C-H stretch bond, which is characteristically present in alkanes. The alkane group is related to cellulose [31].

The peaks at wavenumber 1412.25 cm^{-1}, 1596.25 cm^{-1} and 1590.06 cm^{-1} in Figures 3 and 4 with C=C-C stretch, represent an aromatic compound, which gives an indication of the lignin in both the extracted cellulose and the NaCMC. In addition, by the analysis of the spectrum of the extracted cellulose, peaks of wave number 1314.57 cm^{-1} and 1157.10 cm^{-1} were observed, and this is indicative of the alcohols (cellulose, hemicellulose, and lignin), esters, carboxylic acids, and ether's.

However, by making a comparison between the two spectral graphs, it is observed that there are peaks that fall within the range of 1000 cm^{-1} and 1320 cm^{-1}. This indicates that cellulose, hemicellulose, and lignin are present in both samples. This is because this range in question is attributed to the alcohol and carboxylic acid because of their characteristic C-O stretch bond type.

The peak corresponding to the wave number 894.42 cm^{-1} in Figure 3 shows that there is an aromatic functional group present with a characteristic C-H bond type and indicates the presence of lignin in the extracted sample. This is confirmed with the presence of an alkene group, which is also indicative of the presence of lignin in the sample. From FTIR, it's clear that the cellulose extracted is not a pure form and still needs some further purification.

Impact of Particle Size of Cocoa NaCMC on Filtration Parameters

The variation of the filtration parameters with the particle size of the cocoa NaCMC at high temperature and differential pressure (low and high) condition in a permeable formation is presented in Figures 5 to 7.

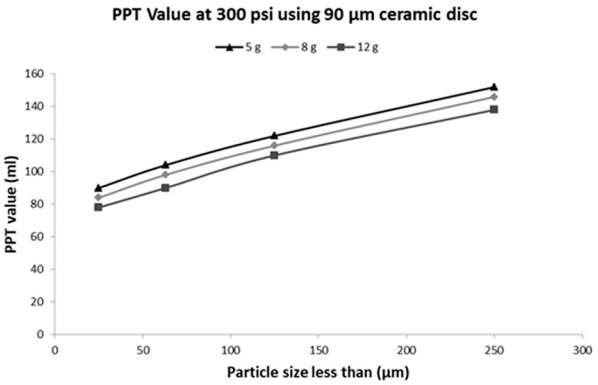

Figure 5: PPT value versus particle sizes of different masses of cocoa NaCMC.

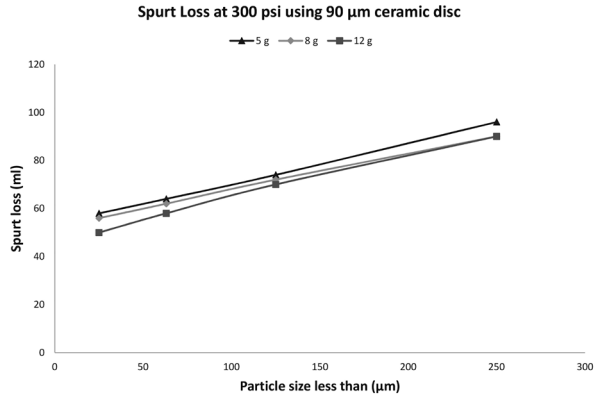

Figure 6: Spurt loss versus particle sizes of different masses of cocoa NaCMC.

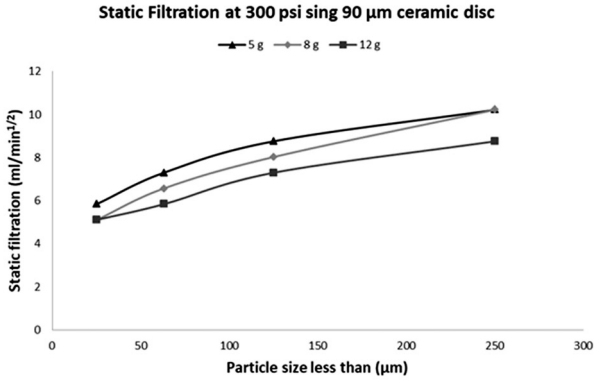

Figure 7: Static filtration versus particle sizes of different masses of cocoa NaCMC.

Filtration parameters from the results presented were improved as the particle size of cocoa NaCMC decreased. From Tables 2 and 3 as well as Tables 4-7 the samples A, B, G, and I exhibited the same trend.

Table 2: High-temperature and low-pressure differential Filtration results of extracted cellulose at 100 psi.

Sample	Mass (g)	Vol $_{7.5\ min}$ (ml)	Vol $_{30\ min}$ (ml)	PPTV (ml)	SL (ml)	SFR (ml/ min$^{1/2}$)
At 100 psi with 10µm ceramic disc						
A	0	40	53	106	54	9.49
B	5	34	44	88	48	7.30
G	5	49	67	134	62	13.14
	8	47	64	128	60	12.41
	12	45	61	122	58	11.68
I	5	45	61	122	58	11.68
	8	42	57	114	54	10.95
	12	40	54	108	52	10.22
At 100 psi with 90µm ceramic disc						
A	0	50	62	124	76	8.76
B	5	41	50	100	64	6.57
G	5	57	75	150	78	13.14
	8	55	72	144	76	12.41
	12	52	69	138	70	12.41
I	5	52	70	140	68	13.14
	8	49	66	132	64	12.41
	12	47	64	128	60	1241

PPTV – Permeability Plugging Tester Value
SL- Spurt loss SF- Static Filtration Rate

Table 3: High-temperature and high-pressure differential filtration results of extracted cellulose at 300psi with different ceramic discs.

Sample	Mass (g)	Vol $_{7.5\ min}$ (ml)	Vol $_{30\ min}$ (ml)	PPTV (ml)	SL (ml)	SFR (ml/ min$^{1/2}$)
At 300 psi with 10µm ceramic disc						
A	0	48	63	126	66	10.95
B	5	42	54	108	60	8.76
G	5	57	77	154	74	14.60
	8	55	74	148	72	13.87
	12	53	71	122	70	13.14
I	5	57	75	150	78	13.14
	8	54	71	142	74	12.41
	12	52	68	136	72	11.68
At 300 psi with 90µm ceramic disc						
A	0	57	74	148	80	12.41
B	5	51	65	130	74	10.22
G	5	66	88	176	88	16.06
	8	64	85	170	86	15.33
	12	62	82	164	84	14.60
I	5	66	86	172	92	14.60
	8	63	82	164	88	13.87
	12	61	79	158	86	13.14

PPTV – Permeability Plugging Tester Value
SL- Spurt loss SF- Static Filtration Rate

Moreover, the same observation is seen in the other formulation samples A, B, C, D, E, and H as shown in Tables 4 to 7.

Table 4: High-temperature and low-pressure differential filtration results of cocoa NaCMC at 100 psi using 10 µm ceramic disc.

Sample	Mass of NaCMC(g)	Vol $_{7.5\ min}$ (ml)	Vol $_{30\ min}$ (ml)	PPTV (ml)	SL (ml)	SFR (ml/min$^{1/2}$)
A	0	40	53	106	54	9.49
B	5	34	44	88	48	7.30
H	5	20	24	48	32	2.92
	8	18	21	42	30	2.19
	12	15	18	36	24	2.19
C	5	25	31	62	38	4.38
	8	23	28	56	36	3.65
	12	20	24	48	32	2.92
D	5	30	38	76	44	5.84
	8	28	35	70	42	5.11
	12	26	32	64	40	4.38
E	5	38	47	94	58	6.57
	8	35	45	90	50	7.30
	12	33	41	82	50	5.84

PPTV: Permeability Plugging Tester Value, SL: Spurt Loss, and SF: Static Filtration Rate.

Table 5: High-temperature and low-pressure differential filtration results of cocoa NaCMC at 100 psi using 90 µm ceramic disc.

Sample	**Weight of NaCMC (g)**	**Vol $_{7.5\ min}$ (ml)**	**Vol $_{30\ min}$ (ml)**	**PPTV (ml)**	**SL (ml)**	**SLR (ml/min$^{1/2}$)**
A	0	50	62	124	76	8.76
B	5	41	50	100	64	6.57
H	5	26	30	60	44	2.92
	8	25	28	56	44	2.19
	12	22	25	50	38	2.19
C	5	32	39	78	50	5.11
	8	30	35	70	50	3.65
	12	27	31	62	48	2.92
D	5	37	45	90	58	5.84
	8	36	43	86	58	5.11
	12	33	40	80	52	5.11
E	5	45	53	106	74	5.84
	8	43	52	104	68	6.57
	12	42	51	102	66	6.57

PPTV: Permeability Plugging Tester Value, SL: Spurt Loss, and SF: Static Filtration Rate.

Table 6: High-temperature and high-pressure differential filtration results cocoa NaCMC at 300 psi using 10 µm ceramic disc.

Sample	Weight of NaCMC (g)	Vol $_{7.5\ min}$ (ml)	Vol $_{30\ min}$ (ml)	PPTV (ml)	SL (ml)	SFR (ml/min$^{1/2}$)
A	0	48	63	126	66	10.95
B	5	42	54	108	60	8.76
H	5	28	34	68	44	4.38
	8	26	31	62	42	3.65
	12	23	28	56	36	3.65
C	5	33	41	82	50	5.84
	8	31	38	76	48	5.11
	12	28	34	68	44	4.38
D	5	40	50	100	60	7.30
	8	38	47	94	58	6.57
	12	36	44	88	56	5.84
E	5	53	65	130	82	8.76
	8	50	62	124	76	8.76
	12	48	58	116	76	7.30

PPTV: Permeability Plugging Tester Value, SL: Spurt Loss, and SF: Static Filtration Rate.

Table 7: High Temperature High pressure differential filtration results of cocoa NaCMC at 300 psi using 90 µm ceramic disc.

Sample	Weight of NaCMC (g)	Vol $_{7.5\ min}$ (ml)	Vol $_{30\ min}$ (ml)	PPTV (ml)	SL (ml)	SFR (ml/min$^{1/2}$)
A	0	57	74	148	88	12.41
B	5	51	65	130	74	10.22
H	5	37	45	90	58	5.84
	8	35	42	84	56	5.11
	12	32	39	78	50	5.11
C	5	42	52	104	64	7.30
	8	40	49	98	62	6.57
	12	37	45	90	58	5.84
D	5	49	61	122	74	8.76
	8	47	58	116	72	8.03
	12	45	55	110	70	7.30
E	5	62	76	152	96	10.22
	8	59	73	146	90	10.22
	12	57	69	138	90	8.76

PPTV: Permeability Plugging Tester Value, SL: Spurt Loss, and SF: Static Filtration Rate.

The main reason for the advent of this trend is improvement of small sized particles by the efficiency of the impermeable filter cake formation. It can be observed from Figure 8 that particle size reduction also results in thinner filter cakes.

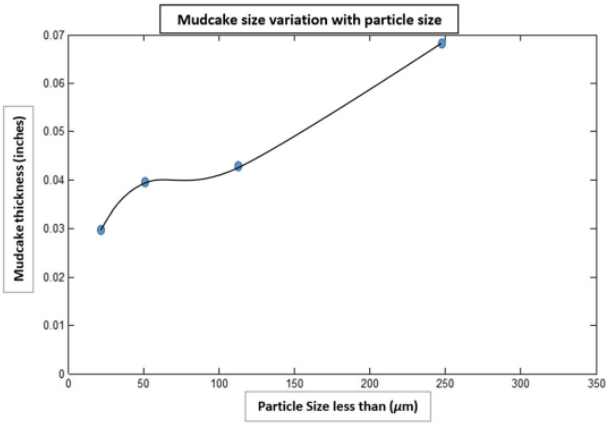

Figure 8: Mud cake size variation with particle size.

This is due to the fact that as filter cake easily becomes impermeable, fewer particles are deposited to increase filter cake size. Small sized particles also have a larger surface area; therefore, they tend to be more resistant to pressure [21]. It is worth noting from Tables 4 to 7 that the cocoa NaCMC have had better filtration parameters in comparison with the industrial PAC even at larger particle sizes. It is only the sample E with NaCMC of particle sizes <250 µm that performed worse than sample B with industrial PAC of particle sizes <25 µm. This can be attributed to the results from SEM test which have shown the strand-like nature of the CMC particles in comparison with the cylindrical nature of the PAC particles.

Impact of the Mass of Cocoa NaCMC on Filtration Parameters

It is evident from Tables 4 to 7 that there is a general decreasing trend in all filtration parameters with an increase in the quantity of cocoa NaCMC in the drilling mud formulation regardless of the size of the particle of the filtration agent used. This trend is also evident from Figures 5 to 7 as the 12-gram curve is always below the 5-gram and 8-gram curves.

This trend and behavior is attributable to the increase in viscosity with increasing quantity of the cocoa NaCMC. Viscosity increase is one of the basic mechanisms which affects filtration; in addition, the more viscous fluid is forced through the filter cake, the lower the filtration rate will be.

With the exception of sample E, all samples with 5 grams of cocoa NaCMC had better filtration parameters than samples with 5 grams of PAC. Moreover, a representative example is seen in Figure 9.

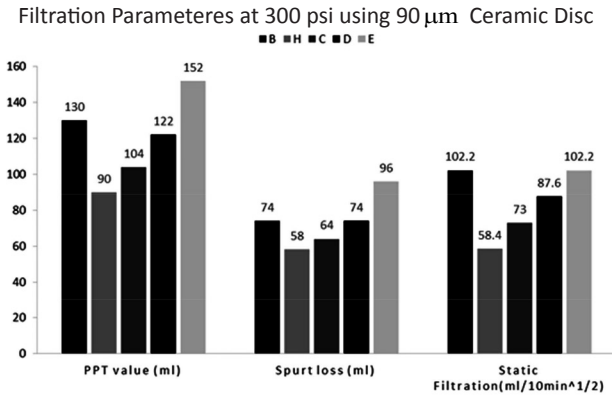

Figure 9: Comparison of Filtration parameters of cocoa NaCMC with industrial PAC.

Filtration Control Performance in Low and High Permeability Formation

The use of the different ceramic discs was to evaluate the performance of the cocoa NaCMC as a filtration agent in formations with different permeability. As a comparison was made between Tables 4, 5, 6, and 7, the general trend was observed, and thereby this trend showed that the filtration control performance declined in higher permeable formation. The trend was profound in the PPT values and the spurt loss but not the static filtration rate.

This trend can be explained in terms of particle bridging which is another basic mechanism that affects filtration. Moreover, particle bridging is more efficient in smaller pores than in larger pores. Also, smaller particles tend to bridge smaller pores while larger particles bridge larger pores. As explained in particles size effect on mud cake formation, smaller particles form more efficient mud cake.

Filtration Control Performance at Different Differential Pressures

Evaluation of filtration characteristics of cocoa NaCMC at different differential pressures is done by comparing Table 4 to Table 6 and Table 5 to Table 7. It was observed that filtration characteristics of the cocoa NaCMC were better at low differential pressures than under high differential pressures. The Differential pressure factor influences particle bridging hence the efficiency of mud cake formation in the wellbore. Mud cake compressibility is another factor that controls filtrate loss. At high differential pressures, larger particles may aid in limiting the solids that plug into pores and reduce the effect of mud cake compaction [32].

Impact of Filtration Agents on the Rheological Properties of Drilling Mud

Pseudoplastic behavior of drilling muds is very essential because a higher viscosity at a low shear rate is required to suspend and move cuttings up to the surface. Moreover, low viscosity is required at higher shear rates for drilling fluids to flow with little counteraction [2]. This behavior is best described with the power law model. The results achieved using Equations 4 to 9 are shown in Table 8.

Table 8: Drilling mud rheological parameters with various filtration agents.

Sample	Parameters of Bingham plastic fluids			Parameters of power law fluids	
	μ_a (cP) / μ_p (cP)	τ_y (lb/100 ft^2)	GS_{10s} / GS_{10min} (lb/100 ft^2)	n (-)	K (lb.s^n/100 ft^2)
A	9.5/6	7	3/9	0.547	0.43
B	27/8	38	3/11	0.231	10.88
H	20/12	16	3/9	0.514	1.13
I	24/57	35	15/25	0.222	10.50

It can be observed that the cocoa NaCMC caused a significant rise in the yield point and viscosity, but the drilling fluid's gel strength was not altered. It is worth noting that the extracted cellulose which didn't possess better filtration characteristics due to its insoluble nature has a better effect on the rheology of the mud.

The plot of shear rate against stress for different samples is presented in Figure 10.

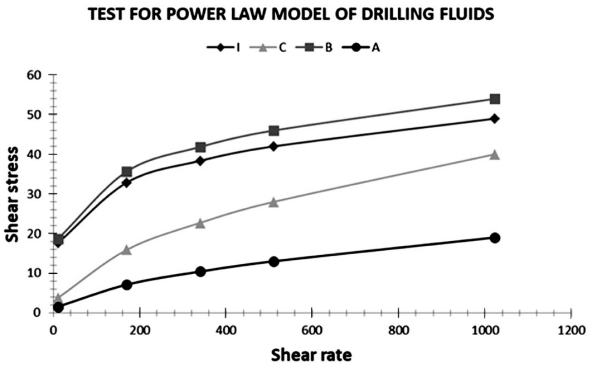

Figure 10: Shear rate against stress for drilling mud samples.

It shows a non-linear relationship which depicts that the drilling fluid samples are pseudoplastic. The values of the flow index (n) as presented in Table 8 for all the samples were less than one (n<1) which also substantiated the fact that the samples were pseudoplastic. The raw drilling fluid without filtration agent had the least consistency index (K)

value and the highest flow index (n) value, which having these indexes means that the samples with the filtration agents are more viscous and more shear thinning.

Morphological and Thermal Degradation Studies

According to Figure 1, it could be said that the working mechanisms for the cocoa CMC would be different from the industrial PAC.

Moreover, according to Figure 1, the cocoa CMCs were strained together in a long continuous path in comparison with the circular spherical path of the industrial PAC. This morphological feature would dictate the cocoa CMC's critical concentration path and agglomeration in a drilling fluid formulation. By the stranding nature, it would take a shorter time for sealing to be achieved especially if the reservoir permeability path is far bigger than the cocoa CMC particle range. The morphology of the synthesized cocoa cellulose also would suggest that in high permeability reservoirs, it should perform as an excellent fluid loss agent in comparison with the PAC due to their continuous dense strand-like nature. This was confirmed with test analysis when the ceramic disk of 90 was utilized with lower fluid loss been for the synthesized cocoa NaCMC than the industrial PAC.

Thermogravimetric analysis (TGA) on the cocoa NaCMC showed that the thermal decomposition behavior of the cocoa NaCMC degraded after 175 °C, but more specifically it occurred within the range of 175 and 375 °C. This result was consistent with works also carried out by Asuquo et al and Titiloye et al [33, 34]. Using the conservative figure of 175 °C for analysis, it is noted that the performance of the synthesized product at 175 °C is extremely good since most bio-based synthesized products do not achieve such temperature degradation curve. Figure 2 (a and b) shows 3 differential quantities indicating signatures of the components' regions removed by the thermal degradation process. Based on the signatures, they can be related to the different compositions of the cocoa pod husks thereby allowing for component analysis.

The first stage loss in weight which is the moisture evolution stage has been estimated to be 6%. During the evolution of the volatile component which was about 63% could be attributed to the decomposition of hemicelluloses and cellulose between 175 and 375 °C. It should be stated that FTIR showed that the synthesized CMC was not fully pure and did contain a significant amount of hemicellulose. Thus TGA and DSC confirmed the FTIR results and the need to purify the synthesized material.

CONCLUSIONS

1. The NaCMC prepared from cocoa pod husk was proved to be a better filtration agent at high-temperature conditions and in low and high permeable formations in comparison with the industrial PAC.
2.Thermal stability of the synthesized agro material-cocoa CMC at high temperatures was governed.
3. Increased filtration control was a function of the particle size and mass of the cocoa NaCMC.
4. The cocoa NaCMC also improved the rheology of the drilling mud and proved to make the drilling fluid more pseudoplastic.
5. Finally, FTIR and TGA showed that the CMC from cocoa husk still was not pure cellulose and needed some more purification. Moreover, further purification of cellulose should improve the current rheological results.

NOMENCLATURES

CMC	: Carboxymethyl Cellulose
NaCMC	: Sodium Carboxymethyl Cellulose
PPTV	: Permeability Plugging Tester Value
SL	: Spurt Loss
SF	: Static Filtration Rate
SFR	: Static filtration Rate
PPTV	: Permeability plugging tester value
μ_α	: Apparent viscosity
μ_p	: Plastic viscosity
τ_y	: Yield point

Appendix 1: Conversion of Cocoa Husk into Cellulose.

Read Pictures From Top Left: A- Fresh cocoa pods crushed into smaller sizes. B-blended powder sieved using the RETSCH Sieve Analysis Machine. C- Water bath used for CMC synthesis. D-powder dissolved in 2% w/v sodium hydroxide (NaOH) in a beaker. The resulting mixture was heated in a water bath at 80 °C for 3 hours and was thoroughly washed under distilled water until the pH was approximately neutral. E- Bleaching process with 500 ml Mirazone bleach containing 7% of sodium hypochlorite at 80 °C under mechanical stirring for 15 minutes. F- Mixture treated with 1L 12% w/v NaOH solution and heated at 80 °C for an hour. G- Final bleaching was done to remove remaining lignin and hemicellulose and also to purify the cellulose. H- The extracted cellulose was cleaned thoroughly using deionized water for 2 hours. I-Cellulose after putting in an oven (Memmert, UFE800) set at 60 °C for 24 hours.

Appendix 2: Synthesis of Cocoa Sodium Carboxymethyl Cellulose from Raw Cocoa Cellulose.

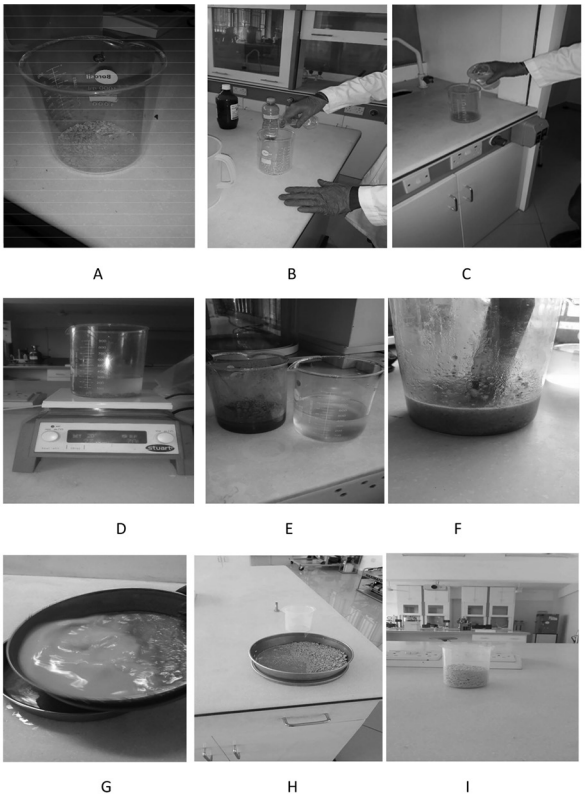

Read Pictures From Top Left: A- Raw cocoa husk cellulose. B- NaOH and isopropanol needed for the first stage of conversion C- Addition of NaOH and isopropanol to 45 grams of the extracted cellulose in a beaker. D- The mixture mechanically stirred and allowed to stand for 30 minutes at room

temperature. E- 10.8g of sodium monochloroacetic acid added to the pre-treated cellulose. F- Continuous stirring before the mixture was covered with aluminum foil and kept in a Memmert oven UFE800 at 55 °C for 180 minutes. G- The slurry of the mixture was neutralized with glacial acetic acid and then filtered. H-The sodium carboxymethyl cellulose produced was washed with 300 ml of ethanol to remove undesirable salts, followed by a methanol wash to remove remaining impurities and the water was evaporated using a Memmert oven UFE800 at 55 °C for an hour. I- Final converted sodium carboxymethyl cellulose.

REFERENCES

1. BAKER H., "Drilling Fluids Reference Manual," (2nd ed), Texas, Baker Hughes, **2006**, 1-775.
2. Maghrabi S., Smith D., Engel A., Henry J., and et al., "Design and Development of a Novel Fluid Loss Additive for Invert Emulsion Drilling Fluids from a Renewable Raw Material," *Society of Petroleum Engineers*, **2019**.
3. Rosato M. J. and Supriyono A., "Polymer Fluid-Loss Agent Aids Well Cleanouts," *Society of Petroleum Engineers*, **2003**,
4. Jouenne S., Chakibi H., and Levitt D., "Polymer Stability after Successive Mechanical-Degradation Events," Society of Petroleum Engineers, **2018.**
5. Jia H., Chen H., and Guo S., "Fluid Loss Control Mechanism of Using Polymer Gel Pill Based on Multi-crosslinking during Overbalanced Well Workover and Completion," *Fuel Journal*, **2017**, *210*, 207–216.
6. Davoodi S., Ramazani S. A., Jamshidi S., and Fellah Jahromi A., "A Novel Field Applicable Mud Formula with Enhanced Fluid Loss Properties in High Pressure-High Temperature Well Condition Containing Pistachio Shell Powder," *Journal of Petroleum Science and Engineering*, **2018**, *162*, 378–385.
7. Agwu O. E. and Akpabio J. U., "Using Agro-waste Materials as Possible Filter Loss Control Agents in Drilling Muds: A Review," *Journal of Petroleum Science and Engineering*, **2018**, *163*, 185–198.
8. Ezeakacha C. P. and Salehi S., "Experimental and Statistical Investigation of Drilling Fluid Loss in Porous Media: Part 2 (Fractures)," *Journal of Natural Gas Science and Engineeing*, **2019**, *51*, 257–266.
9. Caenn R. and Chillingar G. V., "Drilling Fluids State of the Art," *Journal of Petroleum Science and Engineering*, ***1996***, *14*, 221–230.
10. Song K., Wu Q., Li M., Wojtanowicz A. K., and et al., "Performance of Low Solid Bentonite Drilling Fluids Modified by Cellulose Nanoparticles," *Journal of Natural Gas Science and Engineering*, **2016**, *34*, 1403-1411.
11. Abdo J. and Haneef M. D., "Clay nanoparticles Modified Drilling Fluids for Drilling of Deep Hydrocarbon Wells," *Applied Clay Science*, **2013**, *86*, 76–82.
12. Abdo J., Zaier R., Hassan E., Al-sharji H., and Al-shabibi A., "ZnO–clay Nanocomposites for Enhance Drilling at HTHP Conditions," **2014**, *46*, 970–974.
13. Heggset E. B., Chinga-carrasco G., and Syverud K., "Temperature Stability of Nanocellulose Dispersions. Carbohydr Polymer," **2017**, *157*, 114–121.
14. Johann P. P., "Water-Based Muds Using Synthetic Polymers Developed For High-Temperature

Drilling," *Oil Gas Journal*, **1992**, *90*, 40–45.
15. Pushpamalar V., Langford S. J., Ahmad M., and Lim Y. Y., "Optimization of Reaction Conditions for Preparing Carboxymethyl Cellulose from Sago Waste," **2006**, *64*, 312–318.
16. Azizi A., Shahrul M., Ibrahim N., and et al., "Agarwood Waste as A New Fluid Loss Control Agent in Water-based Drilling Fluid," *International Journal of Science and Engineering*, **2013**, *5*, 101–105.
17. Ghazali N. A., Alias N. H., Mohd T. A. T., and Noorsuhana M. Y., "Potential of Corn Starch as Fluid Loss Control Agent in Drilling Mud," *Applied Mechanics and Materials*, **2015**, *754*, 682-687.
18. Alsabagh A. M., Abdou M. I., Ahmed H. E. S., Khalil A. A. S., and et al., "Evaluation of Some Natural Water-insoluble Cellulosic Material as Lost Circulation Control Additives in Water-Based Drilling Fluid," *Egyptian Journal of Petroleum*, **2015**, *24*, 461–468.
19. Kafashi S., Rasaei M., and Karimi G., "Effects of Sugarcane and Polyanionic Cellulose on Rheological Properties of Drilling Mud: An Experimental Approach," *Egyptian Journal of Petroleum*, **2017**, *26*, 371–374.
20. Onuh C. Y., Igwilo K. C., Anawe P. A. L., Olakunle D., and Omotoke O., "Environmentally Friendly Fluid loss Control Agent in Water-Based Mud for Oil and Gas Drilling Operations," *International Journal of Applied Engineering Research*, **2017**, *12*, 1520-1523.
21. Haider S., Zine M., Boureghda M., Aknouche H., Akkouche A., and Hammadi L., "An Ecological Water-based Drilling Mud (WBM) with Low Cost: Substitution of Polymers by Wood Wastes," *Journal of Petroleum Exploration and Production Technology*, **2018**, *9*(1), 307-313.
22. Hutomo G. S., Marseno D. W., and Anggrahini S., "Synthesis and Characterization of Sodium Carboxymethylcellulose from Pod Husk of Cacao (Theobroma cacao L .)," *African Journal of Food Science,* **2012**, *6*(6), 180-185.
23. Thomas D. C., "Thermal Stability of Starch- and Carboxymethyl Cellulose-Based Polymers Used in Drilling Fluids," *Society of Petroleum Engineers*, **1982**.
24. Drilling Fluids–Specifications and Testing (18th ed.), *American Petroleum Institute*, API 13B-1, **2010**, 1-22.
25. Dick M. A., Heinz T. J., Svoboda C. F., and Aston M., "Optimizing the Selection of Bridging Particles for Reservoir Drilling Fluids," *Society of Petroleum Engineers*, **2000**.
26. Bourgoyne A. T., Millheim K. K., Chenevert M. E., and et al., "Applied Drilling Engineering Chapter 8 Solutions," *Society of Petroleum Engineers*, **1986**.
27. Coates J., "Interpretation of Infrared Spectra, A Practical Approach (Meyers ed.)," Encyclopedia of Analytical Chemistry, *John Wiley and Sons Ltd*., **2000**, 10815–10837.
28. Bakri M. K. and Jayamani E., "Comparative Study of Functional Groups In Natural Fibers: Fourier Transform Infrared Analysis (FTIR)," International Conference on Futuristic Trends in *Engineering, Science, Humanities, and Technology* (FTESHT-16), **2016**.
29. Bourgoyne A. T., Millheim K. K., Chenevert M. E., and Young F. S., "Applied Drilling Engineering Chapter 8 Solutions," *Society of Petroleum Engineers*, **1986**.

30. Coates J., "Interpretation of Infrared Spectra, A Practical Approach (Meyers ed.)," Encyclopedia of Analytical Chemistry, *John Wiley and Sons Ltd*., **2000**, 10815–10837.
31. Bakri M. K. and Jayamani E., "Comparative Study Of Functional Groups In Natural Fibers: Fourier Transform Infrared Analysis (FTIR)," *International Conference on Futuristic Trends in Engineering, Science*, Humanities, and Technology (FTESHT-16), **2016**.
32. He W., and Stephens M. P., "Bridging Particle Size Distribution in Drilling Fluid and Formation Damage," *Society of Petroleum Engineers*, **2011**.
33. Asuquo E. D. and Martin A. D., "Sorption of Cadmium (II) Ion from Aqueous Solution onto Sweet Potato (Ipomoea batatas L.) Peel Adsorbent: Characterisation, Kinetic and Isotherm Studies," *Journal of Environmental Chemistry and Engineering*, **2016**, *4*, 4207–4228.
34. Titiloye J. O., Bakar M. S. A., and Odetoye T. E., "Thermochemical Characterisation of Agricultural Wastes from West Africa," *Industrial Crops Production*, **2013**, *47*, 199–203.